Sensor noise modeling using the Skellam distribution: Application to the color edge detection

Youngbae Hwang
Dept. of Electrical Engineering
KAIST
Daejeon, Korea
unicorn@rcv.kaist.ac.kr

Jun-Sik Kim
Robotics Institute
Carnegie Mellon University
Pittsburgh, PA, USA
kimjs@ri.cmu.edu

In-So Kweon
Dept. of Electrical Engineering
KAIST
Daejeon, Korea
iskweon@kaist.ac.kr

Abstract

In this paper, we introduce the Skellam distribution as a sensor noise model for CCD or CMOS cameras. This is derived from the Poisson distribution of photons that determine the sensor response. We show that the Skellam distribution can be used to measure the intensity difference of pixels in the spatial domain, as well as in the temporal domain. In addition, we show that Skellam parameters are linearly related to the intensity of the pixels. This property means that the brighter pixels tolerate greater variation of intensity than the darker pixels. This enables us to decide automatically whether two pixels have different colors. We apply this modeling to detect the edges in color images. The resulting algorithm requires only a confidence interval for a hypothesis test, because it uses the distribution of image noise directly. More importantly, we demonstrate that without conventional Gaussian smoothing the noise model-based approach can automatically extract the fine details of image structures, such as edges and corners, independent of camera setting.

1. Introduction

Noise is inevitable in any image capturing process. In the computer vision community, various noise modeling methods have been proposed for two or more images. However, there are few studies dealing with noise modeling in a single image. In general, most low-level processing methods, which must treat the noise in a single image, try to reduce the noise instead of modeling it. The conventional strategy for extracting features, such as corners and edges, is to preprocess the images with Gaussian kernels so as to suppress the image noise by smoothing [3, 5]. However, because the Gaussian smoothing diminishes the details in the image, as well as the image noise, the result may miss important parts of the scene structure. In addition, although Gaussian parameters for smoothing must be determined properly, the effect of Gaussian smoothing previously has only been considered in a few studies.

Many methods have been proposed to determine whether the difference between two pixels is caused by noise or scene changes between two different images. Rosin [11] used the Gaussian and the Poisson distribution for noise modeling in the temporal and the spatial domain, respectively. Ohta [10] assumed that noise in pixels follows the Gaussian distribution in a temporal domain. A Gaussian distribution as a noise model is widely used, but there have been alternative methods using new noise models that include various distributions [2, 8]. Bazi *et al*. [2] applied the generalized Gaussian model to separate changed and unchanged regions in log-ratio SAR images. Hwang *et al*. [8] proposed the generalized exponential model to detect changes in images captured by common CCD cameras.

On the other hand, there have been studies that endeavor to estimate the image noise based on camera imaging processes. As stated in [6], there are five main noise sources, including fixed pattern noise, dark current noise, and shot noise. Healey showed that the intensity and variance of the noise are statistically linear. Most image noise modeling requires two or more images because it is difficult to determine the true brightness. Liu *et al*. [9] recently proposed a noise estimation method from a single image. They defined a noise level function as the variance of the standard deviation of noise with respect to image intensity. After learning the space of the noise level function, which means how the noise level changes with brightness, they use Bayesian MAP estimation to infer the noise level function from a single image.

In this paper, we introduce the Skellam distribution as the sensor noise model. This is derived from the Poisson distribution of photons, which determine the sensor response. The noise modeling based on the Skellam distribution has been used before in the context of PET imaging [14], but

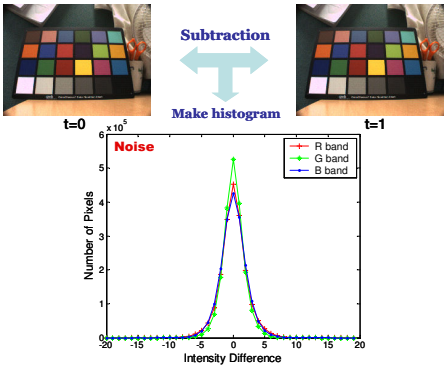

Figure 1. The histogram of intensity difference between two consecutive images

to our knowledge, it has not been used for natural images. We propose a method for Skellam parameter estimation. It does not require the complicated prior knowledge, such as a set of camera response functions and explicit color segmentation, which is mandatory for the previous work [9]. We show that our noise modeling is exactly fit for noise distributions in images captured by CCD cameras. We find the important property that intensity is linearly related to the Skellam parameters. From this, more importantly, we can determine an exact noise distribution for each pixel according to its intensity value, whereas the work of Liu *et al*. [9] estimates the upper bounds of the noise levels. We can apply our noise modeling to detect edges with a given confidence interval as a hypothesis test. The proposed edge detector not only suppresses the image noise effectively, but also detects fine details of image structures.

The remainder of this paper is organized as follows. In Section 2, we describe our model of image noise using the Skellam distribution and the properties of the Skellam distribution. Section 3 describes the noise statistics estimation strategy using the Skellam parameters. In Section 4, we apply our noise modeling to color edge detection. We summarize our work in Section 5.

2. The Skellam distribution as image noise

Figure 1 shows the histogram of the intensity difference between two consecutive images in a single channel. Although there is no scene change, the differences have the distribution shape shown in Figure 1 due to the effect of noise. In [15], several sources of image noise are listed, but most of the sources can usually be considerably reduced by appropriate design of manufacturer. They may also be ignored, because the total SNR of a complete system is typically dominated by the smallest SNR; the most dominant noise component is photon noise in CCD or CMOS cameras. The number of photons is governed by the laws of quantum physics, which means that we cannot know the true intensity because of the uncertainty in the number of photons; this is called photon noise. Because it is caused by the fundamental statistical nature of photons, we cannot remove or reduce this noise. The photon noise is usually modeled by a Poisson distribution [15]. We assume that the noise shown in Figure 1 is caused by the dominant photon noise.

2.1. The Skellam distribution for noise modeling of intensity difference

When we assume that the image intensity of each pixel follows the Poisson distribution, the probability distribution for p photons in an observation time interval T s is known to be a Poisson distribution because:

$$P(p \mid \rho, T) = \frac{(\rho T)^p e^{-\rho T}}{p!} \tag{1}$$

where ρ is the rate parameter, measured in photons per second. The mean and standard deviation are:

$$\mu = \rho T \tag{2}$$

$$\sigma = \sqrt{\rho T} \tag{3}$$

Because the number of photons determines the intensity of a pixel, photon noise is not independent of the signal. In addition, photon noise is neither Gaussian nor additive. As shown in (2), μ means the number of photons over an interval T. It is natural that the number of photons in a brighter pixel is greater than that in a darker pixel. From this we can predict that μ will increase as the brightness or intensity increases. This prediction is verified in the next section.

If μ is sufficiently large, we can approximate a Poisson distribution as a Gaussian distribution [7]. Therefore, the intensity difference distribution also follows a Gaussian distribution, because it is the difference between two Gaussian random variables; however, μ differs with intensity. This means that for darker pixels, the Gaussian approximation may be invalid.

We use a Poisson distribution to represent the intensity difference distribution to avoid the erroneous Gaussian approximation. The difference between two Poisson random variables is defined as a Skellam distribution [12]. The probability mass function (pmf) of a Skellam distribution is a function of k, which means the difference between two Poisson random variables. It is expressed as:

$$f(k; \mu_1, \mu_2) = e^{-(\mu_1+\mu_2)} \left(\frac{\mu_1}{\mu_2}\right)^{k/2} I_k(2\sqrt{\mu_1 \mu_2}) \tag{4}$$

where μ_1 and μ_2 are the means, or expected values, of the two Poisson distributions, and $I_k(z)$ is the modified Bessel function of the first kind. Examples of pmfs for Skellam distributions are shown in Figure 2.

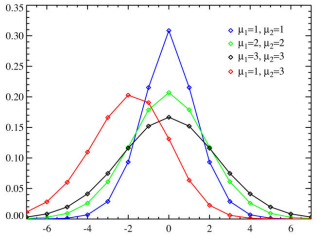

Figure 2. Examples of the pmf for the Skellam distribution[13]

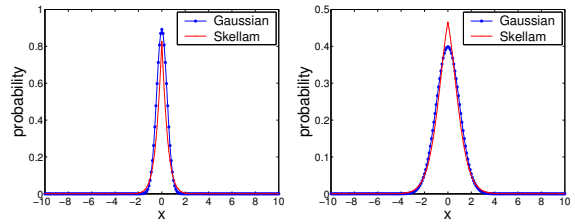

(a) $\mu_1 = \mu_2 = 0.1, \sigma = 0.2$ (b) $\mu_1 = \mu_2 = 0.5, \sigma = 1.0$

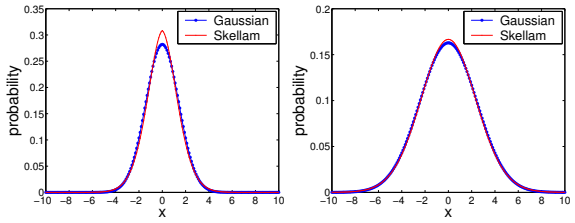

(c) $\mu_1 = \mu_2 = 1.0, \sigma = 2.0$ (d) $\mu_1 = \mu_2 = 3.0, \sigma = 6.0$

Figure 3. Comparison of the Skellam and the Gaussian distributions

2.2. The properties of the Skellam distribution

For the special case when $\mu_1 = \mu_2$, a Skellam distribution tends to a Gaussian distribution for large μ and k [1]. Because both μ and k are not sufficiently large for low-intensity pixels, we cannot approximate the Skellam distribution by a Gaussian distribution. Figure 3 shows the difference between the Skellam and the Gaussian distributions as a function of μ_1 and μ_2.

We can estimate the Skellam parameters of intensity difference by using the statistics of the Skellam distributions. The mean μ_S and variance σ_S^2 of a Skellam distribution are given by:

$$\mu_S = \mu_1 - \mu_2 \tag{5}$$

$$\sigma_S^2 = \mu_1 + \mu_2 \tag{6}$$

From (5) and (6), we calculate the parameters μ_1 and μ_2 directly as:

$$\mu_1 = \frac{\mu_S + \sigma_S^2}{2} \tag{7}$$

$$\mu_2 = \frac{-\mu_S + \sigma_S^2}{2} \tag{8}$$

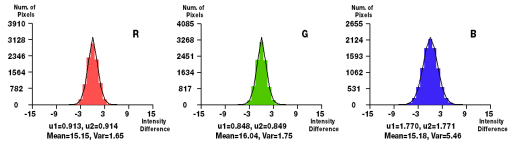

(a) Black patch (24th patch)

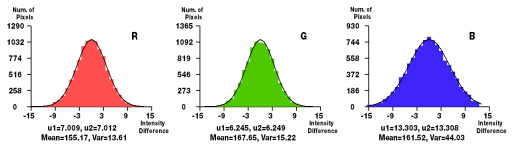

(b) Gray patch (21th patch)

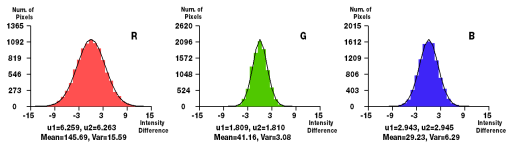

(c) Red patch (15th patch)

Figure 4. Skellam parameter estimation using 10,000 static images

μ_S and σ_S^2 are obtained from images of a static scene as:

$$\mu_S = \frac{\sum_t (x_t(i,j) - x_{t+1}(i,j))}{n} \tag{9}$$

$$\sigma_S^2 = \frac{\sum_t (\mu_S - (x_t(i,j) - x_{t+1}(i,j))^2}{n} \tag{10}$$

where $x_t(i,j)$ denotes the intensity of the (i,j) position for frame t and n is the number of total images. To estimate Skellam parameters for various colors, we captured 10,000 images of a static scene of Gretag Macbeth ColorChecker using a Pointgrey Scorpion camera (image resolution of 1,600 x 1,200 pixels, exposure time of 1/15 s). The estimation results are as shown in Figure 4. The parameters of the Skellam distribution are different for each patch. In particular, a black patch has low Skellam parameters and a gray patch has high Skellam parameters, as expected. These are expected because μ_1 and μ_2 are the numbers of photons in the CCD cells during the capture time.

Figure 4 shows another important verification. By Skellam modeling, we can estimate the distribution of intensity difference accurately. This shows that our assumption of dominant photon noise is appropriate.

We applied our Skellam modeling scheme to a large number of static images. In many cases, it was not possible to capture a large number of images from a static camera. To make our modeling more general, we should be able to estimate noise from a single image. We assume that each pixel in a spatial domain is mutually independent, which means that the noise distribution along the spatial domain is the same as that along the temporal domain. To verify our assumption, we compared the noise distribution in the spatial domain with that in the temporal domain. We obtained

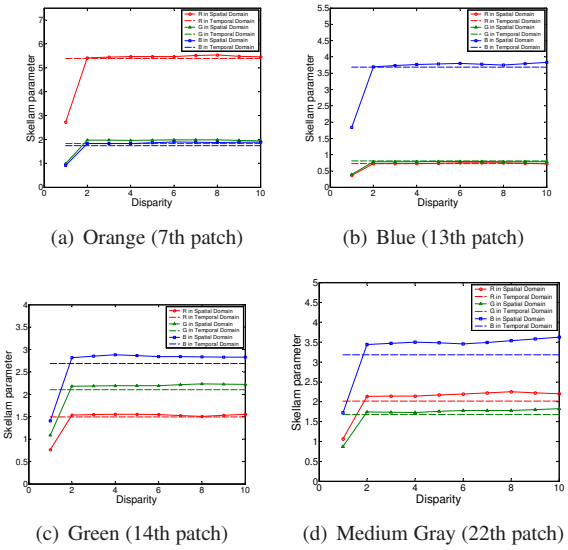

(a) Orange (7th patch) (b) Blue (13th patch)

(c) Green (14th patch) (d) Medium Gray (22th patch)

Figure 5. Comparison of the Skellam parameters in the spatial and the temporal domain

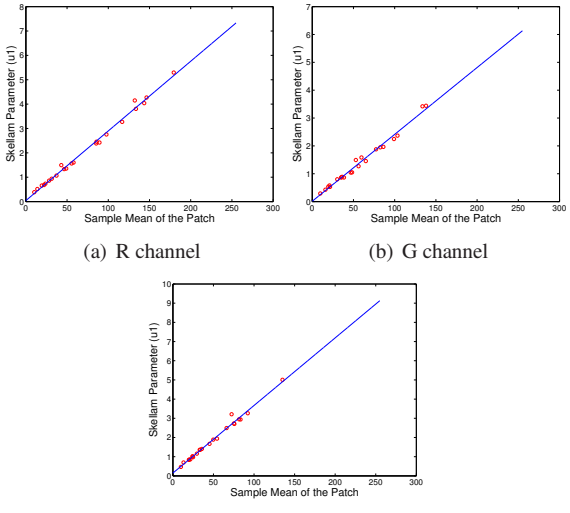

(a) R channel (b) G channel

(c) B channel

Figure 6. Linearity between sample means and the Skellam parameters

the modeling results in the temporal domain using (9) and (10). To estimate the noise in the spatial domain, we cut homogeneous color patches in a pattern image shown in Figure 1. Using the patches, we applied our modeling strategy to the spatial domain based on the following equations:

$$\mu_S = \frac{\sum_{(i,j)\in P}(x_t(i,j) - x_t(i+d_x, j+d_y))}{n} \quad (11)$$

$$\sigma_S^2 = \frac{\sum_{(i,j)\in P}(\mu_S - (x_t(i,j) - x_t(i+d_x, j+d_y))^2}{n} \quad (12)$$

where $(i,j) \in P$ means all points in the patch, d_x and d_y are disparities in the horizontal and vertical direction, respectively, and n is the total number of pixels in the patch.

Figure 5 shows the comparison of the modeling results from the spatial and the temporal domains. We used a Pointgrey Scorpion camera (image resolution of 1,600 x 1,200 pixels, exposure time of 1/7.5 s). From Figure 5, we verified that the Skellam parameters in the temporal and the spatial domain are similar. This shows that the difference of intensity is an ergodic process. Note that the Skellam parameters are smaller than the other estimation results when the disparity is one. We found that derives from the demosaicing process, which is the reconstruction of three colors at every pixel from the single-color samples measured by the Bayer filter array of the CCD. When we tested using a 3CCD camera that does not require demosaicing, such as the HITACHI HV-F22, there were no such effects. There are slight differences in the results in the temporal and the spatial domain because we selected only one pixel in the patch when we estimated the distribution in the temporal domain. Depending on which pixel is selected in the patch, there will be a small variation in the Skellam parameters. Although we only increased the horizontal disparity, d_x, from one to 10 in this experiment, the result from the vertical disparity variation displays a similar result. Because the proposed modeling scheme satisfies the ergodic requirement, we can apply our modeling to single image applications.

3. Noise statistics estimation using the Skellam parameter

In the previous section, we showed that Skellam modeling is applicable in the spatial domain, as well as in the temporal domain. However, there is another problem in applying our modeling to a single image, because a sufficient number of pixels in the homogeneous patch are necessary to estimate the Skellam parameters. We derive another important property to expand our modeling scheme to a single pixel.

3.1. Linearity between intensity and the Skellam parameters of patches

We assume that there should be a parametric relation between Skellam parameters and intensity. From a single pixel, we cannot extract meaningful statistics for a mean or variance. To show the relationship between the intensity and the Skellam parameters, we excised 24 color patches from the image of a pattern shown in Figure 1. We drew a scatter plot of a Skellam parameter with respect to a sample mean at each patch in Figure 6. Figure 6 shows the

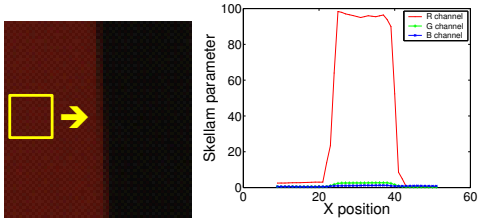

(a) Mask is moving (b) Skellam parameters

Figure 7. The variation of the Skellam parameters at the edge

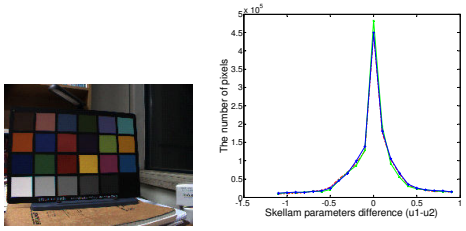

(a) Test image (b) The histogram of $\mu_1 - \mu_2$ for each channel

Figure 8. The histogram of the difference between Skellam parameters

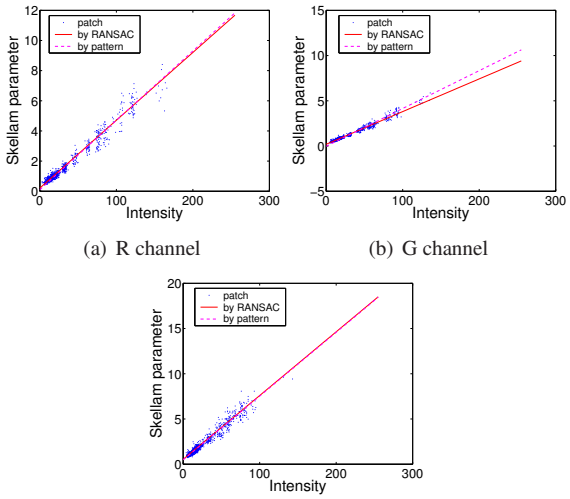

(a) R channel (b) G channel

(c) B channel

Figure 9. Results of the Intensity-Skellam line estimation

linear relationship between the sample means and Skellam parameters. We call this line an Intensity-Skellam line. We assume that a pixel value can be approximated by a sample mean and that we can estimate its Skellam parameters when we have the Intensity-Skellam lines. The lines in Figure 6 only change with camera gain, not scene radiance or illumination. Once the Intensity-Skellam line has been determined, we can use the line without modification provided the gain is fixed.

3.2. Estimation of the Intensity-Skellam line in a single image

The estimation of an Intensity-Skellam line requires patches that have homogeneous colors, as shown in fitting a line in Figure 6; however, finding a homogeneous patch is not trivial. Conventional approaches use color segmentation to locate homogeneous regions, as in [9], but the segmentation is also difficult. Instead, we use the properties of the Skellam parameters to select appropriate patches. The Skellam mean is calculated as the mean of the intensity difference of neighboring pixels in (11). Transitions of colors between neighboring pixels leads to the movement of the Skellam mean, as shown in Figure 7. We verified this using a red-black transition patch. As the patch moves to the left, the Skellam parameters become larger when the patch contains a transition part.

When an image is captured under directional illumination, the Skellam mean at the patch may be shifted slightly although that patch has a homogeneous scene color. To accommodate this, we first construct a histogram of Skellam means. By finding a peak of the histogram of Skellam means, we overcome the mean shift effect. Although the illumination was located in an upward position, the mean of the Skellam parameters shifted only slightly in our experiments. Figure 8(b) shows the histogram of Skellam means for the input image of Figure 8(a).

We easily determine the peak and use patches that have a Skellam mean close to the peak. The Intensity-Skellam parameter pair of patches are not on a single line due to Skellam parameter variation. In addition, some outliers are not removed by filtering. We apply a simple RANSAC algorithm to determine the line because it is certain that the distribution of patches is dense at the center. As such, we obtain a good fit for the line. The patches used are randomly selected to reduce time complexity. We selected 1,000 19 x 19 patches. Figure 9 shows the result of the estimation. For its evaluation, we drew a line obtained by manual color pattern segmentation. Although we used a small part of the patches, our estimated lines are accurate in that we cannot discriminate between the estimated lines and those obtained by the pattern.

3.3. Determination of an intensity allowance

Because we have Skellam parameters for each intensity value, we have exact noise distributions based on the Skellam parameters. Based on these distributions, we can determine an allowance for intensity variation due to the sensor noise. Our strategy for determining an intensity allowance is to test a hypothesis given a confidence interval.

In order to test a hypothesis, we must have a cumulative distribution function (cdf). Because the pmf of a Skellam

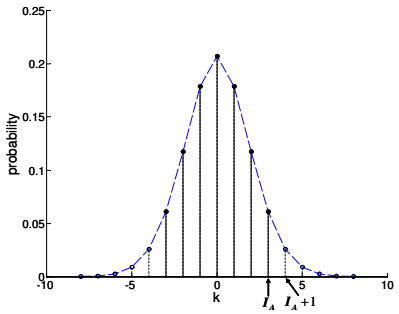

Figure 10. Intensity allowance given the pmf ($1-\alpha$ = sum of the length of solid lines, α = sum of the length of dotted lines. Refer text.)

distribution is defined only at integer values, we can calculate the cdf as:

$$F(K;\mu_1,\mu_2) = \sum_{k=-\infty}^{K} e^{-(\mu_1+\mu_2)} \left(\frac{\mu_1}{\mu_2}\right)^{k/2} I_k(2\sqrt{\mu_1\mu_2}) \tag{13}$$

The acceptance region for a critical value, I, is:

$$A(I) = \{v|v < I\} = F(I;\mu_1,\mu_2) - F(-I;\mu_1,\mu_2). \tag{14}$$

We determine the intensity allowance I_A, that is, the critical value, as:

$$I_A = \arg\max_I A(I) \quad \text{s.t. } A(I) \le 1-\alpha \tag{15}$$

where α is the size of the type I error, shown in Figure 10, which is a true rejection rate with a $(1-\alpha)*100\%$ confidence interval [4].

4. Application to edge detection based on the proposed noise modeling

We apply our noise modeling to edge detection because we can use the estimated intensity allowance directly. Most edge detectors smooth the image with Gaussian kernels as a preprocessing step to suppress the image noise. However, an edge detector based on our noise modeling does not smooth images because we know the exact range of intensity variation due to sensor noise. In spite of having no Gaussian smoothing, the proposed edge detector not only finds detailed edges, but also suppresses the noise in the image.

4.1. Edge detection and postprocessing

Our edge detection is simple because we have the exact intensity allowance based on noise estimation using a Skellam distribution. The strategy for our edge detection is very similar to that of a change detection with two consecutive images. If the difference between two neighboring pixels is within the intensity allowance, there is no edge; otherwise, there must be a real change of scene colors, which means an edge. The edge measure in both the horizontal and vertical directions is defined as:

$$e_x^c(i,j) = \frac{|x^c(i-1,j) - x^c(i+1,j)| - I_A}{I_A} \tag{16}$$

$$e_y^c(i,j) = \frac{|x^c(i,j-1) - x^c(i,j+1)| - I_A}{I_A} \tag{17}$$

where I_A denotes the intensity allowance at the pixel and c is the color channels, which are r, g, and b in RGB color space. The edge measure measures the normalized distance of intensity from the intensity allowance. If all horizontal and vertical edge measures are negative, that pixel is regarded as a nonedge pixel. Otherwise, we sum all the horizontal and vertical edge measures. Consequently, the total edge measure of a pixel is:

$$e(i,j) = \begin{cases} 0, & \text{if } \begin{cases} e_x^c(i,j) < 0 \\ e_y^c(i,j) < 0 \end{cases} \text{ for all } c \\ \sum_c e_x^c(i,j) + \sum_c e_y^c(i,j), & \text{otherwise} \end{cases} \tag{18}$$

This edge measure preemptively suppresses the edge measure due to sensor noise.

When the edge measures for all pixels are calculated, we apply nonmaximum suppression because real edges do not correspond to a single line. In [3], two values are required for a hysteresis thresholding to link edges after nonmaximum suppression. However, we regard the pixels that have nonzero edge measures as being edge pixels because the intensity difference exceeds the intensity allowance determined from the noise distributions.

4.2. Edge detection results

Figure 11 shows the normalized edge measure in various illumination conditions. The normalized edge measure is the initial step of edge detection followed by further processing, such as non-maximum suppression and hysteresis linking. Therefore, the correctness of the normalized edge measure is very crucial for edge detection. We compared the results using the proposed method with 99% confidence interval and those from the Canny operator with low and high thresholds, which are fixed for all input images. The results from the Canny operator not only cannot reduce the false edges caused by image noise, but also cannot detect find details as shown in the dark illuminated image (second input image). Our proposed method outperforms the results from the Canny operator. Without any parameter changes, our method reduce the noise correctly and detect edges even in the very dark environment. In addition, the detection of the red number 5 is difficult using the Canny operator,

whereas our method detect it with the almost same amount of edge measures of other numbers because our method combines the color information effectively.

Figure 12 shows the edge detection results. Our proposed edge detector has only one parameter, which is the confidence interval. A Canny edge detector [3] has three parameters: a scale for Gaussian smoothing, and a low and a high threshold for hysteresis linking. Determining the values is case-sensitive and critical to the performance. In Figure 12, we compared the results using the proposed method and the various outputs from the Canny edge detector in MATLAB with various scales and thresholds. Our proposed method outperforms the Canny edge results. It suppresses most of the false edges shown in Canny's results with the medium or the automatic threshold. Furthermore, our result shows the fine details of the edges. The common problem of conventional edges is inaccurate localization around the corner because of smoothing. As shown in the magnification view of the corner, the localization of edges around the corner using our method is well-preserved, whereas it was inferior for the Canny edge detector with a scale of smoothing sufficiently high to suppress all the unexpected edges due to image noise. This is possible because our threshold is determined separately for each pixel from the estimated noise distribution.

5. Conclusion

Image noise has been conventionally regarded as an additive Gaussian random variable. However, the Gaussian noise model is not applicable in general, especially in regions of low intensity.

In this paper, we introduce a Skellam distribution as a sensor noise model for CCD or CMOS cameras. The Skellam distribution is defined as the difference between two Poisson random variables that describe the photon noise in images. We show that the Skellam model describes the process well in all intensity ranges. The Skellam noise model has two important properties; first, it is applicable in the spatial domain, as well as in the temporal domain. Using this property, we can estimate the distribution of noise from a single image, whereas most noise estimation methods require multiple images. Furthermore, the Skellam parameters can be determined from the sample mean and the sample variance of the image, assuming homogeneity. The second property is that there is a linear relationship between intensity and the Skellam parameters represented by an Intensity-Skellam line, which is only dependent on the gains of the cameras. Because the Skellam parameters completely determine the noise distribution of pixel intensity, the allowance in intensity variation due to the sensor noise is determined by the intensity of only one pixel.

As an application of the proposed noise model, we propose a simple color edge detector. Because the intensity

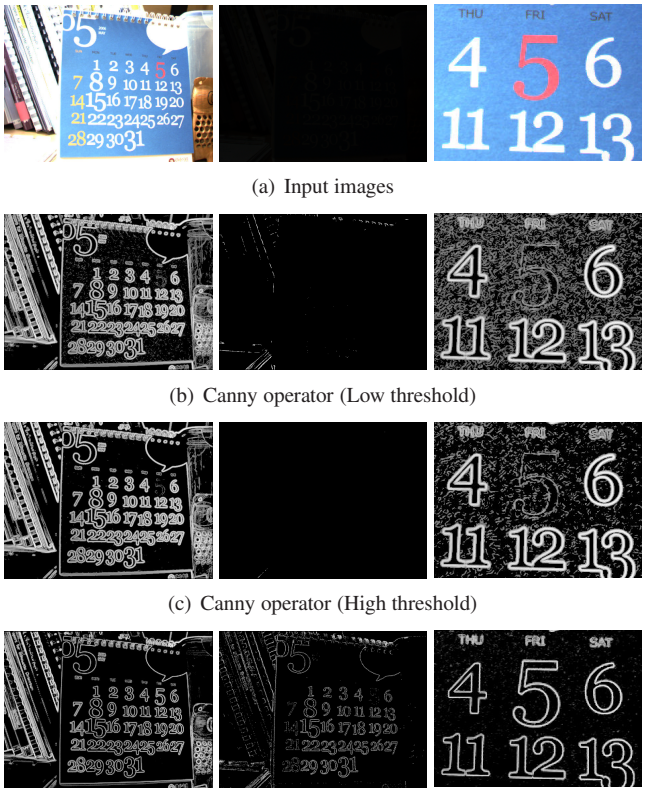

(a) Input images

(b) Canny operator (Low threshold)

(c) Canny operator (High threshold)

(d) Proposed method (99% confidence interval)

Figure 11. Normalized edge measure in various illumination conditions

allowance is known from an image, neighboring pixels that have intensities greater than the allowance are regarded as edges, similar to the change detection in the time domain. Experiments show that the proposed method can detect fine details in the image structures, as well as suppress the noise effect without Gaussian smoothing.

Acknowledgements

This research has been partially supported by the Korean MOST for NRL Program (Grant number M1-0302-00-0064), by the MIC for the project, "Development of Cooperative Network-based Humanoids' Technology" of Korea, and by Agency for Defense Development.

References

[1] M. Abramowitz and I. A. Stegun. *Handbook of mathematical functions with formulars, graphs, and mathematical tables*. New York: Dover, 1972.

[2] Y. Bazi, L. Bruzzone, and F. Melgani. An unsupervised approach based on the generalized gaussian model to automatic change detection in multitemporal sar images. *IEEE Trans. on Geo. and Remote Sensing*, 12(1):874–887, 2005.

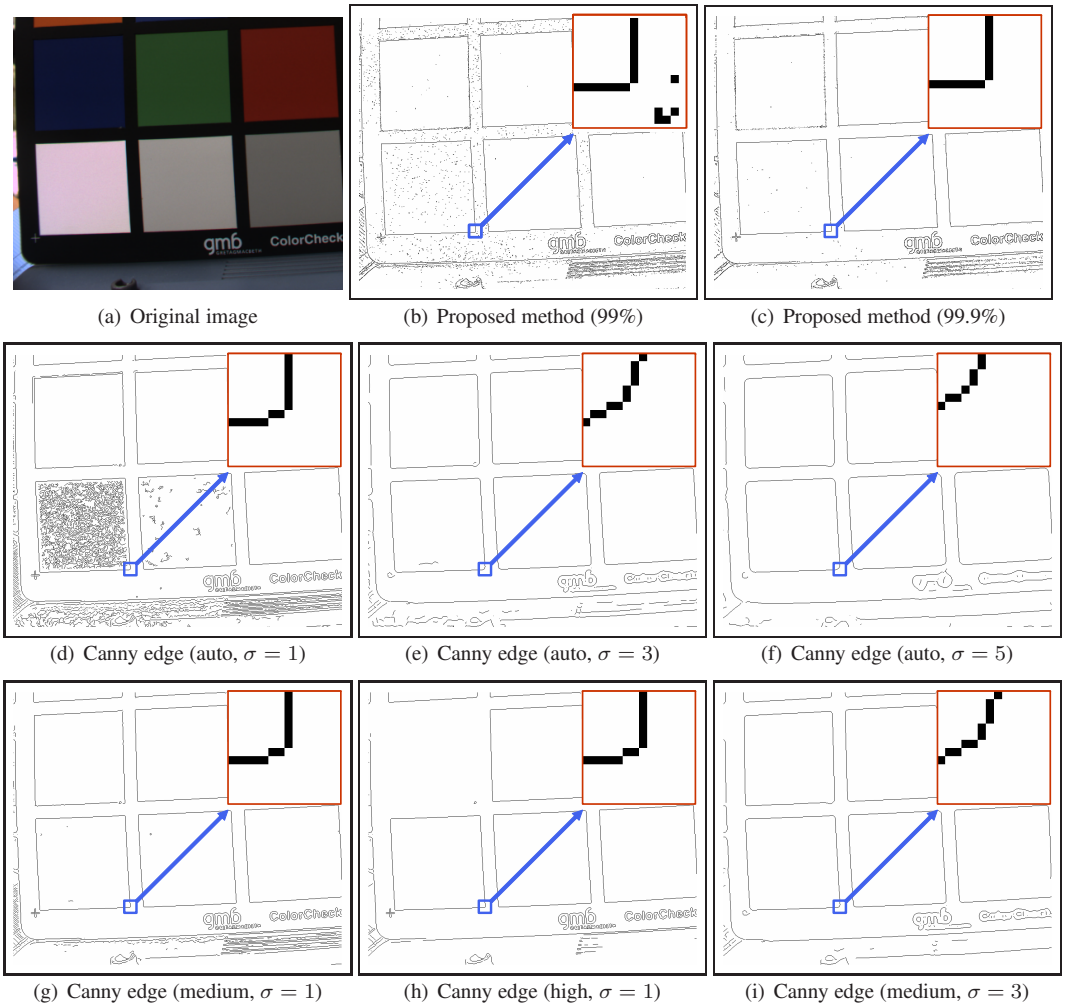

(a) Original image (b) Proposed method (99%) (c) Proposed method (99.9%)

(d) Canny edge (auto, $\sigma = 1$) (e) Canny edge (auto, $\sigma = 3$) (f) Canny edge (auto, $\sigma = 5$)

(g) Canny edge (medium, $\sigma = 1$) (h) Canny edge (high, $\sigma = 1$) (i) Canny edge (medium, $\sigma = 3$)

Figure 12. Edge detection results compared with Canny edge using parameter settings; automatic threshold=(0.0063, 0.0156), medium threshold=(0.025, 0.035) and high threshold=(0.065, 0.075) in normalized intensity

[3] J. Canny. A computational approach to edge detection. *IEEE Trans. on Pattern Analysis and Machine Intelligence*, 8(6):679–698, 1986.

[4] E. R. Dougherty. *Probability and statistics for the engineering, computing and physical sciences*. Prentice Hall, 1990.

[5] C. Harris and M. Stephens. A combined corner and edge detector. In *Fourth Alvey Vision Conference*, pages 147–151, 1988.

[6] G. E. Healey and R. Kondepudy. Radiometric ccd camera calibration and noise estimation. *IEEE Trans. on Pattern Analysis and Machine Intelligence*, 16(3):267–276, 1994.

[7] W. M. Hubbard. The approximation of a poisson distribution by a gaussian distribution. *Proceedings of the IEEE*, 58:1374–1375, 1970.

[8] Y. Hwang, J. S. Kim, and I. Kweon. Change detection using a statistical model of the noise in color images. In *Int. Conf. Intelligent Robots and System*, pages 274–279, 1998.

[9] C. Liu, W. T. Freeman, R. Szeliski, and S. B. Kang. Noise estimation from a single image. In *Int. conf. Computer Vision and Pattern Recognition*, pages 901–908, 2006.

[10] N. Ohta. A statistical approach to background subtraction for surveillance systems. In *Int. Conf. Computer Vision*, pages 481–486, 2001.

[11] P. L. Rosin. Thresholding for change detection. In *Int. Conf. Computer Vision*, pages 274–279, 1998.

[12] J. G. Skellam. The frequency distribution of the difference between two poisson variates belonging to different populations. *Journal of the Royal Statistical Society: Series A*, 109(3):296, 1946.

[13] Wikipedia. Skellam distribution — wikipedia, the free encyclopedia.

[14] M. Yavuz and J. A. Fessler. Maximum likelihood emission image reconstruction for randoms-precorrected pet scans. In *IEEE Nuclear Science Symposium Conference Record*, pages 15/229–15/233, 2000.

[15] I. Young, J. Gerbrands, and L. van Vliet. Fundamentals of image processing, 1995. Delft University of Technology.